Ice-sheet collapse and sea-level rise at the Bølling warming 14,600 years ago

Citation for published version:
Deschamps, P, Durand, N, Bard, E, Hamelin, B, Camoin, G, Thomas, AL, Henderson, GM, Okuno, J & Yokoyama, Y 2012, 'Ice-sheet collapse and sea-level rise at the Bølling warming 14,600 years ago', *Nature*, vol. 483, no. 7391, pp. 559-564. https://doi.org/10.1038/nature10902

Digital Object Identifier (DOI):
10.1038/nature10902

Published In:
Nature

DOI: 10.1038/nature10902

Ice-sheet collapse and sea-level rise at the Bølling warming 14,600 years ago

Pierre Deschamps*, Nicolas Durand, Edouard Bard, Bruno Hamelin, Gilbert Camoin, Alexander L. Thomas, Gideon M. Henderson, Jun'ichi Okuno and Yusuke Yokoyama

*Corresponding Author.

Ice sheet collapse and sea-level rise at the Bølling warming, 14,600 yr ago

Past sea-level records provide invaluable information about the response of ice sheets to climate forcing. Some such records suggest that the last deglaciation was punctuated by a dramatic period of sea-level rise, of ~20 meters in less than 500 years. Controversy about the amplitude and timing of this meltwater pulse (MWP-1A) has, however, led to uncertainty about the source of the meltwater and its temporal and causal relationship with abrupt climate changes of the deglaciation. Here, we present U-Th ages of corals drilled offshore Tahiti during IODP Expedition 310. We provide tight constraints on the timing of MWP-1A, which started after 14.65 kyr BP and ended before 14.31 kyr BP, making it coeval with the Bølling warming. The amplitude of the event at Tahiti is constrained to between 12 and 22 m, with a most probable value between 14 and 18 m. This range implies that the rate of eustatic rise exceeded 40 mm/yr during this dramatic event, and featured significant meltwater from the southern hemisphere.

Although dynamic responses to climate forcing in the Greenland and Antarctic ice sheets may already contribute to present-day sea-level rise, projections of sea-level change for the 21st century do not fully include potential changes in ice dynamics. As acknowledged by the IPCC, the vulnerability of Greenland and Antarctica to ongoing warming and related discharge feedbacks remains a major source of uncertainty in projected sea-level rise. Reconstructions of past sea-level changes have provided evidence for large amplitude and rapid discharges of freshwater from continental ice sheets. Several sea-level records suggest that the glacioeustatic rise following the Last Glacial Maximum (LGM) was characterized by brief periods of extremely rapid sea-level rise. These short-term events, referred to as Melt

Water Pulses (MWPs), likely disturbed oceanic thermohaline circulation and global climate during the last deglaciation. The exact chronology, origin, and consequence of these icesheet melting episodes remain unclear. But understanding these episodes is of the utmost importance when considering current uncertainty surrounding potential collapse of large ice sheets in response to recent climate change.

The most extreme deglacial event, termed MWP-1A, was initially identified in the coral-based sea-level record from Barbados5, where a sea-level rise of ~20 meters was inferred between 14.1 and 13.6 ka6. However, this event remains mysterious. Several records bear witness to its occurrence, although no broad agreement has emerged regarding its timing. Due to this lack of consensus, the temporal relationship between MWP-1A and abrupt (millennial-timescale) climatic events that punctuated the last deglaciation are the subject of considerable debate. Additionally, the location(s) of melting ice responsible for this prominent feature of the last deglaciation remains elusive.

Two conflicting scenarios have been proposed to link the timing and source(s) of MWP-1A to the climatic history of the last deglaciation. On the basis of the Barbados record's chronology, it was initially argued that this episode of rapid sea-level rise was caused by a partial melting of Northern Hemispheric Ice Sheets (NHIS). This "Northern" scenario was consistent with a coupled ocean-atmosphere GCM where massive freshwater input to the North Atlantic would result in a weakening of the Atlantic Meridional Overturning Circulation (AMOC) and, through the reduction of deepwater formation in Nordic Seas, the rapid cooling of the Northern Hemisphere. In this scenario, MWP-1A may have initiated the Older Dryas cold event that abruptly ended the Bølling warming ca. 14.1 ka.

In contrast, an alternative scenario points toward an Antarctic ice sheet as the source of MWP-1A and suggests a causative coupling between MWP-1A and the Bølling-Allerød warm period. This “Southern” scenario suggests that MWP-1A coincided with an intensification of the thermohaline circulation at the onset of the Bølling-Allerød warm period, rather than a slowdown during the following cold event as predicted by the “Northern” scenario. The “Southern” scenario was supported by output from a GCM model of intermediate complexity showing that a MWP-1A originating from the West Antarctica Ice Sheet (WAIS) may have triggered sudden reactivation of the AMOC to lead to the Bølling warming. Although still contentious, this scenario solves the apparent conundrum of the Bølling warming by providing a plausible triggering mechanism for the onset of this event, traditionally considered as marking the termination of the last glacial period.

The Tahiti record

Here, we report U-Th dating of coral samples collected from the Tahiti reef slope during the Integrated Ocean Drilling Program (IODP) Expedition 310 “Tahiti Sea-level”. Tahiti is a far field site located at a considerable distance from major former ice sheets and is characterised by slow and regular subsidence rates (0.25 mm/yr, see Supplemental Information - SI).

Previous reconstructions of the deglacial sea-level rise were established from holes drilled onshore through the modern barrier-reef in front of Papeete harbour. The record was continuous from 13.9 ka to present, but did not reach the critical MWP-1A period. A specific target of Expedition 310 was the extension of the previous Tahiti sea-level record to cover earlier portions of the deglaciation. This was performed by offshore drilling of the Tahitian fore-reef slopes seaward of the present-day barrier reef (Fig. 1). These coring operations recovered more than 400 m of post-glacial reef material, ranging from 122 to 40 m below modern sea level (mbsl) in three distinct areas (Maraa, Faaa, and Tiarei) around Tahiti (Fig. 1).

Our reconstruction of sea level relies on absolute U-Th dating of corals, belonging to coralgal assemblages indicative of a range of modern reef environments from the shallow reef crest to the deepest reef slope. Eighty U-Th ages were determined on coral samples recovered from twenty-three holes drilled at fourteen different sites. These new data extend the Tahiti record to cover the last 16 ka (Figure 2), and provide a complete and detailed record of sealevel rise during this key period of the last deglaciation. In each hole, all of the ages are in stratigraphic order (Fig. S2). However, even for the closely-spaced holes, significant differences in recorded water depths may be observed (see for example the difference recorded between Site M0024 versus Site M0009 that may be up to ~10 m; Fig. S2). The depth distribution observed for the various coral species analyzed here is broadly consistent with their present-day biological zonation (Fig. S4). The large number of holes drilled in the fore-reef slope, as well as their widespread distribution, ensured the recovery of the depth distribution of reefal diversity and varying responses of reef development to sea-level rise.

Our observations compare favourably with a reef accretion model proposed by Blanchon and Blakeway, suggesting heterogeneous reef development induced by multiple factors including: spatially random (patchy) colonization; varying accretion patterns; and rugged topography of the pre-glacial surface that partially controlled the post-glacial reef initiation and growth following flooding. Our record, based on several contemporaneous holes, is therefore more representative than a record derived from a single drill hole which may provide a misleading impression of reef response to sea-level rise.

The sea-level rise during early deglaciation

The two oldest samples, dated at 15.74 ± 0.03 ka and 16.09 ± 0.04 ka BP (hereafter all ages are thousand years -ka- Before Present where Present refers to A.D. 1950), are robust branching *Pocillopora* collected at the interface of the underlying Pleistocene unit in cores 24A-15R and 9B-15R. These samples belong to a shallow-water coralgal assemblage (< 10 m) and indicate a RSL of 117 - 107 m during that time. This RSL estimate is strengthened by the presence of an encrusting *Montipora* collected at a subsidence-corrected depth of 114 mbsl in core 25B-11R. Dated at 15.31 ± 0.02 ka, this sample is associated with vermetid gastropods that are indicative of very shallow environment (< ~5 m). From these observations, we may infer a 117 - 109 mbsl RSL during the early part of the deglaciation at Tahiti (see Fig. 2).

Because of glacial isostatic adjustment (GIA), the RSL records from different sites cannot be compared directly, even in far-field regions. For the 14 - 20 ka time window, GIA models produce RSL that is lower at Tahiti than eustatic sea level, in contrast to other sites commonly used for the analysis of sea-level change (Barbados, Bonaparte Gulf and Huon Peninsula) where GIA effects lead to local sea level lying above the eustatic value. By taking this factor into account, our 117 - 109 mbsl RSL estimate at 16 ka is therefore in good agreement with observations from the Sunda Shelf (Fig. S5) for the same period. RSL observations from Barbados and Bonaparte Gulf display a dense cluster of samples dated at about 18 - 19 ka, which strongly constrains eustatic sea level to a depth less than 110 mbsl in this interval. Therefore, a comparison with our data suggests that, during the early stage of deglaciation, after 19 ka MWP, the ESL remained stable or rose only slightly during the time span surrounding the Heinrich 1 event (likely no more than 5 m for ca. 3 ka).

For the time window spanning 16.1 to 14.6 ka, hole 24A (from the outer ridge at Tiarei) delineates the lower envelope of sea-level change. In this hole, coralgal assemblages are indicative of a very shallow environment and were able to keep pace with rising sea level during this period. The pre-MWP-1A RSL is well constrained by three corals samples collected at a subsidence-corrected depth of 105 mbsl: a massive *Montipora* sample dated at

14.65 ± 0.02 ka in core 15A-37R from Maraa; and two robust branching *Pocillopora* samples dated at 14.58 ± 0.05 ka and 14.61 ± 0.03 ka in core 24A-10R from Tiarei (see SI). These two latter corals belong to a coralgal assemblage that typifies a shallow-water environment of less than 10 meters and are associated with vermetids that are indicative of shallow-water conditions (< ~5 m).

The earliest bound for the initiation of the MWP-1A jump is likely within the time range given by those three samples (14.58 - 14.65 ka). Moreover, the two Pocillopora samples dated at 14.58 and 14.61 ka could have grown already at a reasonable water depth (up to 5 m). Thus, they may have already accommodated a part of the sea-level rise related to MWP-1A, implying that the MWP-1A inception could have occurred somewhat earlier (see the upper bound of the shaded area in Fig. 2). The maximum in age for the onset of MWP-1A could thus be close to the oldest of these 3 corals, dated at 14.65 ka. It must be emphasized that this only provides us the uppermost limit for the onset of MWP-1A and we cannot rule out that the jump may have started significantly later, potentially as young as 14.5 ka (see Fig. S5 in the SI).

Occurrence of MWP-1A

The occurrence of MWP-1A is revealed by a major discontinuity in the upper envelope of the data points in the new Tahiti RSL record (Fig. 2). The next shallowest *in situ* samples in the sequence are two branching *Pocillopora* dated at 14.28 ± 0.02 ka and 14.31 ± 0.04 ka in cores 23B-12R and 23A-13R (see SI). These coral samples, recovered at a subsidence-corrected depth of 88 m, are the first datable corals, showing clear evidence of an in-growth position, to colonize the pre-glacial substratum after the MWP-1A sea-level jump. These samples are critical as they provide the most robust constraint on the MWP-1A timing and clearly indicate that the sea-level jump was complete before 14.31 ka. These data lie on the extension of the general trend depicted by onshore holes (Fig. 2) and highlight a regular, slow rate of sealevel rise after MWP-1A. These corals are associated with vermetids, thus indicating very shallow environment (< ~5 m). We infer a conservative estimate of 88 - 83 mbsl for the post- MWP-1A sea level.

The MWP-1A event also coincides with a major change in reef development strategy, as illustrated by numerous samples dated in all drill holes collected on the outer edge of the fore-reef slopes. Before MWP-1A the reef kept pace with sea level, while a widespread deepening and backstepping occurred after MWP-1A. This change in reef response is coincident with changes in the coralgal assemblage composition, such as in Hole M0024A (see SI, Fig. S3) where shallow-water assemblages, dominated by robust branching *Pocillopora*, massive *Porites* and encrusting *Montipora,* change to branching *Porites* species which typify an environment characterized by moderate energy and light intensity. General features of reef geometry can be simulated with a 2D growth model. This model simulates the overall deepening of the reef sequence that follows occurrence of a rapid sea-level rise and clearly indicates that only holes drilled in the intermediate position between the outer ridge and the modern barrier reef are capable of capturing the sea-level position immediately following MWP-1A (see Fig. S9&10). This result probably explains the difficulty encountered by previous onshore or offshore drilling programs (Barbados or Tahiti) to collect shallow-species coral samples that document precisely the end of MWP-1A. The IODP Mission Specific Platform overcame this difficulty by specifically targeting the reefal structures located in intermediate position between the fore-reef slope and the present barrier reef, especially at the Tiarei Site.

Amplitude and duration of MWP-1A at Tahiti

Based on the most conservative estimates deduced above for the pre- and post-MWP-1A sea level, we infer a 17 m amplitude for the sea-level jump, with lowest and uppermost bounds of 12 and 22 m. Several arguments, discussed in detail in the SI, suggest that this range may reasonably be narrowed down to 14 to 18 m, with a median value of 16 m.

In view of the lower and upper limits of the MWP-1A chronozone (14.31 ka and 14.65 ka respectively), the longest possible duration of the jump is ca 350 years (Fig. 3). Considering the median value of 16 m for the local amplitude of MWP–1A at Tahiti, we infer an average RSL rate of ~ 46 ± 6 mm/yr at Tahiti. However, owing to the age uncertainty associated with its inception and termination (see SI), the MWP-1A duration could have been even shorter than this estimate. An extremely sharp meltwater outburst, on the order of a century or less, is thus possible, in which case the 46 mm/yr rate of sea-level rise must be considered as a minimum value.

Timing of MWP-1A

The new MWP-1A chronozone inferred from the extended Tahiti record (i.e. 14.65 to 14.31 ka or shorter, Fig. 3) does not overlap with that previously proposed based on the Barbados record (14.08 ± 0.06 to 13.63 ± 0.03 ka, using the most recent updated data set published by Fairbanks et al.19,29; see SI for a full discussion of this issue).

Several other lines of evidence also suggest that MWP-1A was significantly older than suggested by the Barbados record and, ultimately, concurrent with the Bølling warming. Additional evidence comes from the Sunda Shelf sea-level record, derived from mangrove organic material collected from a shallow siliciclastic platform. This record shows a very sharp sea-level rise dated at a conventional 14C age of 12.42 ± 0.06 ka BP (1 SD, n = 17) coinciding with the 500-year-long 14C plateau that encompasses the Bølling period. Using the IntCal09 calibration curve, the mean calendar age of the MWP-1A event recorded on the Sunda Shelf can be refined to 14.94 - 14.14 ka (2σ interval, see SI for more details regarding this age calculation).

The revised MWP-1A timescale inferred from the new Tahiti record is also coherent with the recent extension of the Huon Peninsula record, where the oldest sample of the post-glacial reef sequence dated at 14.56 ± 0.05 ka places an upper constraint to the end of MWP-1A (Fig. 3). Further indirect evidence is provided by the drowning of coral reefs offshore Hawaii, which occurred at 14.7 ka and has been proposed to be caused by a dramatic increase in sea level related to MWP-1A15.

These records are consistent enough to revise the onset of MWP-1A so it is 500 yrs earlier than the date inferred from the Barbados data. Within this revised timeframe, MWP-1A can no longer be advocated as the trigger for the Older Dryas cooling event that terminated the Bølling period, as proposed previously. Instead, MWP-1A coincided with the inception of the Bølling period (Fig. 3), which has been independently constrained by the GICC 05 Greenland ice core chronology at 14.640 ka (with a maximum counting error of 0.186 ka). The Tahiti record is thus compatible with the idea of a temporal relationship between MWP-1A and Bølling warming. This hypothesis is further substantiated by the concurrent occurrence of rapid flooding on shelf margins and a sea-surface temperature increase in the South China Sea at the Bølling transition.

Source of MWP-1A

Because they account for more than 80% of total sea-level rise during the last deglaciation, NHIS, and especially the Laurentide Ice Sheet (LIS), have commonly been considered as the sole sources for MWP-1A5. Arguments for such a LIS source faced serious objections, however, that led Clark et al. to propose an alternate scenario in which a significant fraction of the meltwater came from Antarctica.

Direct evidence in favour of a northern or southern hemisphere source remains equivocal. Most robust arguments supporting an Antarctic contribution were provided by GIA models. Fingerprinting model experiments demonstrated that comparison of the size of the MWP-1A sea-level rise observed at several sites could provide helpful information about the source(s) of melting ice. Predictions provided by Clark et al. showed that, when melting ice originated exclusively from the LIS, the amplitude of MWP-1A predicted for Barbados should be significantly lower than for far-field sites. This scenario predicted the greatest difference in amplitude between Barbados and Tahiti, with a sea-level rise at Tahiti almost twice that at Barbados.

The 16 m MWP-1A amplitude we assess at Tahiti is comparable to that observed at Sunda (~16 m). At Barbados, the amplitude of the jump must be reassessed on the basis of the re-evaluation of the MWP-1A chronozone. By extrapolating the linear trend defined by hole 12 (Fig. S4), we roughly estimate a ~15 m amplitude of sea-level rise at Barbados. The amplitudes of MWP-1A recorded at these three far-to-intermediate-field sites are thus approximately the same. Following Clark et al.'s predictions, our results seem to preclude a sole LIS contribution to MWP-1A and confirm their preliminary conclusions based solely on the Sunda and Barbados records. On this basis, the Barents and Fennoscandian Ice Sheets can also be considered as possible candidates for the freshwater source (see Fig. 2 in Clark et al.)

but there are several counterarguments to these ice sheets as the major source of freshwater. All other scenarios that provide equal amplitudes of MWP-1A sea-level rise require a significant Antarctic contribution.

These arguments in favour of an AIS contribution were reinforced by GIA predictions conducted by Bassett et al., who showed that the optimal deglacial scenario to fit RSL observations at Barbados, Tahiti, Huon Peninsula and Sunda Shelf during Late glacial time required a MWP-1A with a total amplitude of 23 m, which included an AIS contribution of 15 m with a total NHIS contribution of 8 m (6 m from the LIS).

Using a realistic GIA model (see SI), which uses the earth model proposed by Bassett et al., we performed a new set of simulations that agree well with Bassett's et al. conclusion, pointing towards a substantial AIS contribution. It is difficult at this stage, however, to conclusively determine the relative contributions of NHIS and AIS to MWP-1A because these approaches (fingerprinting and more general GIA modelling) are hampered by uncertainties surrounding the MWP-1A-induced relative sea-level amplitude, especially at the intermediate-field site of Barbados. Following previous studies, which conclude that the MWP-1A amplitude recorded at Tahiti is amplified by 10 to 30% with respect to its eustatic amplitude, our results are consistent with a eustatic MWP-1A rise of roughly ~14 m during the 14.65 - 14.3 ka time window, leading to eustatic sea-level rate of 40 mm/yr. Note that this value is significantly lower than the 20 - 25 m of eustatic rise often reported in the literature. Considering the growing body of evidence suggesting a substantial fraction of MWP-1A originated from Antarctica, it is probable that AIS contributed at least half of the ~14 m eustatic sea-level rise observed during this event. It is worth noting that this estimate of the Antarctic contribution allows us to balance the freshwater budget required for MWP-1A, taking into account the NHIS contributions that have been independently assessed to be between 5 and 10 m equivalent. Recent estimates of AIS contribution to the last deglaciation indicate that its contribution was < 20 m and perhaps lower than 10 - 15 m40-42, implying that a significant, if not the major part of AIS contribution to the last deglaciation, occurred during MWP-1A.

Climatic implications of the revisited MWP-1A history

The IODP "Tahiti Sea Level" Expedition provides significantly improved constraints on MWP-1A timing, demonstrating that MWP-1A should end before 14.3 ka and that it started after 14.65 ka. This makes MWP-1A coeval with the Bølling warming, suggesting a temporal, and likely causal, relationship between these two prominent deglacial features. Owing to the dating uncertainty of the Bølling inception in the Greenland ice record (14.642 ka with maximum counting error of 186 years), it remains difficult to unravel the phasing and causal mechanisms linking the resumption of the AMOC during the Bølling warming and massive meltwater discharges in both hemispheres, through specific atmospheric and oceanic responses. Two end-member scenarios that warrant further investigation can be put forward, however:

The first scenario is that proposed by Weaver at al., based on GCM simulations showing that a rapid freshwater discharge originating from AIS could have led to an intensification of the AMOC. The associated northward ocean heat flux would trigger the Bølling warming in the NH and a rapid melting of LIS. Subsequent studies (e.g. Swingedouw et al. and references therein), however, that have tested Weaver et al.’s scenario showed that the meltwater discharge may have led to competing mechanisms, enhancing or weakening the AMOC, which collectively lead to a subdued climatic response in the NH.

In the second scenario, the phasing of events is reversed, with an initial AMOC increase and associated northward ocean heat transport causing the Bølling warming, which led to rapid melting of NH ice sheets, in particular the LIS. The resulting sea-level rise drove in turn a dramatic collapse of the AIS. Indeed, the Western AIS was partly marine-based during the LGM and thus probably sensitive to the breakup and loss of buttressing ice shelves. In any case, most of the WAIS is characterized by unstable conditions with bedrock below sea level and slopes downward from the margins toward the interior.

Actually, the two scenarios are not mutually exclusive and could have acted in concert during the MWP-1A chronozone, reinforcing each other. They are both compatible with our sea-level and source fingerprinting study, implying that meltwater injections, forming the MWP-1A event, originated from ice sheets in both Antarctica and the NH, including the LIS. In principle, meltwater injection into the North Atlantic could have counteracted the AMOC increase, but the strength of this negative feedback depends on the exact location and mode of meltwater release. Several studies suggested that the LIS meltwater was funnelled through the Mississippi drainage system, before being released in the Gulf of Mexico as a hyperpycnal flow, with a negligible impact on the AMOC.

The two scenarios have similar ingredients but differ by their ultimate trigger, AIS collapse or AMOC increase. These abrupt events could be linked to threshold responses to the Southern Hemisphere gradual warming that occurred under external forcings (orbital and GHG changes) during the early part of the deglaciation.

Much research remains to be done to document the precise sequence of events during the MWP-1A chronozone. This will come from coring coral reefs at other sites (e.g. Barbados, Seychelles), from study of open-ocean sediments in the vicinity of former icesheets, and from modelling work to simulate the complex interplay between ice-sheets, ocean and atmosphere.

Whatever the causes that led to the MWP-1A event and the Bølling warming, and although the total eustatic magnitude of this event is reduced compared to previous estimates, our results prove the existence of a dramatic collapse of past ice sheets at a eustatic rate exceeding 40 mm/yr (at least four time as large as the average deglacial sealevel rise of ~10 mm/yr, see [24] and SI) with a substantial contribution from Antarctica. Understanding this singular event will shed light on the dynamical behaviour of large ice sheets in response to external forcing or internal perturbation of the climate system. This topic is crucial in the context of the present warming as modern ice sheets have been shown to be contributing directly to the recent acceleration in sea-level rise.

Methods Summary

Prior to U-Th dating, rigorous mineralogical and isotopic screening criteria were applied to discard coral samples that suffered any post-mortem diagenetic alteration of their aragonite skeleton. In particular, using X-ray diffraction, we made an effort to improve the detection and quantification of a very small amount of secondary calcite. Coral samples showing more than a 1% calcite content were discarded. Most of the U-Th analyses were performed using a VG-54 thermo-ionisation mass spectrometer equipped with a 30-cm electrostatic analyzer and a pulse-counting Daly detector at CEREGE (see SI for data and analytical issues). The initial (234U/238U)0 values calculated for post-glacial samples yielded a mean value of 1.1458 ± 0.0020 (2σ), falling within the most recent determinations of modern seawater and corals. Additionally, for corals of the same age, (234U/238U)0 values were highly consistent (i.e. within an analytical uncertainty determined for the entire course of the study of 0.8‰, 2σ), and within the larger range adopted by Reimer et al. for isotopic screening criterion in the 0-17 ka interval ((234U/238U)0 = 1.1452 ± 0.0048, 2σ). The clustering of (234U/238U)0 values determined in this study substantially narrows the uncertainty for the evolution of the seawater value through time compared to previous datasets (Vanuatu, Papua New Guinea, and Barbados) that have encompassed the last deglaciation, highlighting the outstanding quality of the coral samples recovered in Tahiti offshore holes. Complementary and duplicated analyses were also performed by MC-ICPMS at Oxford and show a general good agreement within measurement uncertainties.

References

1 Milne, G. A., Gehrels, W. R., Hughes, C. W. & Tamisiea, M. E. Identifying the causes of sea-level change. *Nature Geoscience* **2**, 471-478 (2009).

2 Pfeffer, W. T., Harper, J. T. & O'Neel, S. Kinematic constraints on glacier contributions to 21st-century sea-level rise. *Science* **321**, 1340-1343 (2008).

3 Meehl, G. A. *et al*. in *Climate Change 2007: The Physical Science Basis. Contribution of Working Group I to the Fourth Assessment Report of the Intergovernmental Panel on Climate Change* (eds S. Solomon *et al.*) 747–845 (Cambridge University Press, Cambridge, UK, 2007).

4 Alley, R. B., Clark, P. U., Huybrechts, P. & Joughin, I. Ice-Sheet and Sea-Level Changes. *Science* **310**, 456-460 (2005).

5 Fairbanks, R. G. A 17,000-year glacio-eustatic sea level record; influence of glacial melting rates on the Younger Dryas event and deep-ocean circulation. *Nature* **342**, 637-642 (1989).

6 Bard, E., Hamelin, B. & Fairbanks, R. G. U-Th Ages Obtained by Mass-Spectrometry in Corals from Barbados - Sea-Level During the Past 130,000 Years. *Nature* **346**, 456-458 (1990).

7 Blanchon, P. & Shaw, J. Reef drowning during the last deglaciation - evidence for catastrophic sea-level rise and ice-sheet collapse. *Geology* **23**, 4-8 (1995).

8 Hanebuth, T., Stattegger, K. & Grootes, P. M. Rapid flooding of the sunda shelf: a late-glacial sea-level record. *Science* **288**, 1033-1035 (2000).

9 Yokoyama, Y., Lambeck, K., De Deckker, P., Johnston, P. & Fifield, L. K. Timing of the Last Glacial Maximum from observed sea-level minima. *Nature* **406**, 713-716 (2000).

10 Clark, P. U., McCabe, A. M., Mix, A. C. & Weaver, A. J. Rapid rise of sea level 19,000 years ago and its global implications. *Science* **304**, 1141-1144 (2004).

11 Manabe, S. & Stouffer, R. J. Simulation of Abrupt Climate-Change Induced by Fresh-Water Input to the North-Atlantic Ocean. *Nature* **378**, 165-167 (1995).

12 Weaver, A. J., Saenko, O. A., Clark, P. U. & Mitrovica, J. X. Meltwater pulse 1A from Antarctica as a trigger of the bolling-allerod warm interval. *Science* **299**, 1709-1713 (2003).

13 Bamber, J. L., Riva, R. E. M., Vermeersen, B. L. A. & LeBrocq, A. M. Reassessment of the Potential Sea-Level Rise from a Collapse of the West Antarctic Ice Sheet. *Science* **324**, 901-903 (2009).

14 Bard, E. *et al*. Deglacial sea-level record from Tahiti corals and the timing of global meltwater discharge. *Nature* **382**, 241-244 (1996).

15 Webster, J. M. *et al*. Drowning of the - 150 m reef off Hawaii: A casualty of global meltwater pulse 1A? *Geology* **32**, 249-252 (2004).

16 Stanford, J. D. *et al*. Timing of meltwater pulse 1a and climate responses to meltwater injections. *Paleoceanography* **21** (2006).

17 Clark, P. U. *et al*. Origin of the first global meltwater pulse following the last glacial maximum. *Paleoceanography* **11**, 563-577 (1996).

18 Peltier, W. R. On the hemispheric origins of meltwater pulse 1a. *Quaternary Science Reviews* **24**, 1655 (2005).

19 Peltier, W. R. & Fairbanks, R. G. Global glacial ice volume and Last Glacial Maximum duration from an extended Barbados sea level record. *Quaternary Science Reviews* **25**, 3322 (2006).

20 Bassett, S. E., Milne, G. A., Mitrovica, J. X. & Clark, P. U. Ice sheet and solid earth influences on far-field sea-level histories. *Science* **309**, 925-928 (2005).

21 Kienast, M., Hanebuth, T. J. J., Pelejero, C. & Steinke, S. Synchroneity of meltwater pulse 1a and the Bolling warming: New evidence from the South China Sea. *Geology* **31**, 67-70 (2003).

22 McManus, J. F., Francois, R., Gherardi, J. M., Keigwin, L. D. & Brown-Leger, S. Collapse and rapid resumption of Atlantic meridional circulation linked to deglacial climate changes. *Nature* **428**, 834-837 (2004).

23 Camoin, G., Iryu, Y., McInroy, D. & Scientists', E. *Expedition 310*. (Integrated Ocean Drilling Program Management International, 2007).

24 Bard, E., Hamelin, B. & Delanghe-Sabatier, D. Deglacial Meltwater Pulse 1B and Younger Dryas Sea Levels Revisited with Boreholes at Tahiti. *Science* **327**, 1235-1237 (2010).

25 Cabioch, G., Montaggioni, L. F., Faure, G. & Ribaud-Laurenti, A. Reef coralgal assemblages as recorders of paleobathymetry and sea level changes in the Indo-Pacific province. *Quaternary Science Reviews* **18**, 1681-1695 (1999).

26 Blanchon, P. & Blakeway, D. Are catch-up reefs an artefact of coring? *Sedimentology* **50**, 1271-1282 (2003).

27 Milne, G. A. & Mitrovica, J. X. Searching for eustasy in deglacial sea-level histories. *Quaternary Science Reviews* **27**, 2292-2302 (2008).

28 Peltier, W. R. On eustatic sea level history: Last Glacial Maximum to Holocene. *Quaternary Science Reviews* **21**, 377 (2002).

29 Fairbanks, R. G. *et al*. Radiocarbon calibration curve spanning 0 to 50,000 years BP based on paired $^{230}Th/^{234}U/^{238}U$ and ^{14}C dates on pristine corals. *Quaternary Science Reviews* **24**, 1781 (2005).

30 Reimer, P. J. *et al*. Intcal09 and Marine09 Cadiocarbon age calibration curves, 0-50,000 years cal BP. *Radiocarbon* **51**, 1111-1150 (2009).

31 Edwards, R. L. *et al*. A large drop in atmospheric $^{14}C/^{12}C$ and reduced melting in the Younger Dryas, documented with Th-230 ages of corals. *Science* **260**, 962-968 (1993).

32 Cutler, K. B. *et al*. Rapid sea-level fall and deep-ocean temperature change since the last interglacial period. *Earth Planet. Sci. Lett.* **206**, 253-271 (2003).

33 Liu, J. P. & Milliman, J. D. Reconsidering meltwater pulses 1A and 1B: global impacts of rapid sea level rise. *Journal of Ocean University of China* **3**, 183-190 (2004).

34 Rasmussen, T. L. *et al*. A new Greenland ice core chronology for the last glacial termination. *Journal of Geophysical Research* **111** (2006).

35 Peltier, W. R. Ice-age paleotopography. *Science* **265**, 195-201 (1994).

36 Clark, P. U., Mitrovica, J. X., Milne, G. A. & Tamisiea, M. E. Sea-level fingerprinting as a direct test for the source of global meltwater pulse IA. *Science* **295**, 2438-2441 (2002).

37 Bassett, S. E., Milne, G. A., Bentley, M. J. & Huybrechts, P. Modelling Antarctic sea-level data to explore the possibility of a dominant Antarctic contribution to meltwater pulse IA. *Quaternary Science Reviews* **26**, 2113-2127 (2007).

38 Carlson, A. E. Geochemical constraints on the Laurentide Ice Sheet contribution to Meltwater Pulse 1A. *Quaternary Science Reviews* **28**, 1625-1630 (2009).

39 Tarasov, L. & Peltier, W. R. A calibrated deglacial drainage chronology for the North American continent: evidence of an Arctic trigger for the Younger Dryas. *Quaternary Science Reviews* **25**, 659-688 (2006).

40 Clark, P. U. & Mix, A. C. Ice sheets and sea level of the Last Glacial Maximum. *Quaternary Science Reviews* **21**, 1-7 (2002).

41 Denton, G. H. & Hughes, T. J. Reconstructing the Antarctic Ice Sheet at the Last Glacial Maximum. *Quaternary Science Reviews* **21**, 193-202 (2002).

42 Bentley, M. J. The Antarctic palaeo record and its role in improving predictions of future Antarctic Ice Sheet change. *Journal of Quaternary Science* **25**, 5-18 (2010).

43 Swingedouw, D., Fichefet, T., Goosse, H. & Loutre, M. F. Impact of transient freshwater releases in the Southern Ocean on the AMOC and climate. *Climate Dynamics* **33**, 365-381 (2009).

44 Aharon, P. Entrainment of meltwaters in hyperpycnal flows during deglaciation superfloods in the Gulf of Mexico. *Earth Planet. Sci. Lett.* **241**, 260-270 (2006).

45 Roche, D. M., Renssen, H., Weber, S. L. & Goosse, H. Could meltwater pulses have been sneaked unnoticed into the deep ocean during the last glacial? *Geophysical Research Letters* **34** (2007).

46 Tarasov, L. & Peltier, W. R. Arctic freshwater forcing of the Younger Dryas cold reversal. *Nature* **435**, 662-665 (2005).

47 Knorr, G. & Lohmann, G. Southern Ocean origin for the resumption of Atlantic thermohaline circulation during deglaciation. *Nature* **424**, 532-536 (2003).

48 Knorr, G. & Lohmann, G. Rapid transitions in the Atlantic thermohaline circulation triggered by global warming and meltwater during the last deglaciation. *Geochemistry Geophysics Geosystems* **8** (2007).

49 Andersen, M. B. *et al*. The tracing of riverine U in Arctic seawater with very precise $^{234}U/^{238}U$ measurements. *Earth Planet. Sci. Lett.* **259**, 171 (2007).

50 Thomas, A. L. et al. Penultimate Deglacial Sea-Level Timing from Uranium/Thorium Dating of Tahitian Corals. Science 324, 1186-1189 (2009).

End Notes

Supplementary Information contains SI text, Figures S1 to S10 and Table S1.

Acknowledgements We thank the Integrated Ocean Drilling Program and ECORD (European Consortium for Ocean Research Drilling) for drilling offshore Tahiti and the Bremen Core Repository members for organizing the onshore sampling party. The CEREGE group thanks W. Barthelemy for maintaining mass spectrometers; D. Borschneck for help with x-ray diffraction analyses; P. Dussouillez for help with maps; Paleoclimate work at CEREGE is supported by grants from the Comer Science and Education Foundation, the European Science Foundation (EuroMARC), the European Community (Project Past4Future), the Collège de France and the IRD (Institut de Recherche pour le Développement). The Oxford team is supported by UK Natural Environment Research Council grant NE/D001250/1 and the Comer Science and Education Foundation.

Author Contributions G.C., E.B. and B.H. were PIs for the ODP proposal 519 designing this study. P.D. participated to the IODP sampling party. N.D., P.D. and A.L.T. performed U-Th dating of coral samples; N.D. performed XRD analyses and reef growth modelling simulations; J.O. and Y.Y. performed geophysical modelling simulations; P.D. wrote the manuscript in collaboration with E.B. and B.H. The paper was refined by contributions from N.D., A.L.T., G.M.H. and G.C.

Figure Legends

Figure 1: A Landsat image of Tahiti island showing the location of the three areas (Tiarei, Maraa and Faaa) drilled during IODP Expedition 310 "Tahiti Sea Level" as well as the Papeete harbour where onshore holes were drilled previously. A total of 37 boreholes were cored during IODP 310 at 22 different sites providing more than 400 m of post-glacial reef material[23]. The insets show the bathymetry for each site with the location of the different drilled holes.

Figure 2: (a) Tahiti sea-level curve reconstructed from U-Th dated corals recovered in long holes drilled onshore and offshore the Tahiti Island. Coral depths are expressed in meters below present sea level and are corrected for a constant subsidence rate of 0.25 mm/yr (see SI). Grey symbols correspond to coral samples collected in onshore holes[14,24], whereas coloured symbols correspond to samples collected in offshore holes drilled during the IODP Expedition 310. Red diamonds represent key samples from the inner ridge of Tiarei (Site M0023). The thick blue line represents the lower estimate of the Tahiti RSL curve (see SI). It extends the brown curve determined by linear fits of onshore sea-level data[24] and clearly indicates the occurrence of the MWP-1A event. The shaded time window highlights the tight chronological constraints derived for MWP-1A from the Tahiti record. (b) Blow-up of the MWP-1A time window. The vertical bars reported for each coral sample correspond to their optimal bathymetric habitat range inferred from the coralgal assemblage identification (see SI) and thick orange bars indicate samples associated to vermetid gastropods that are indicative of shallow environment (0-5 m). The

ranges of uncertainty estimated from the bathymetric range of coralgal assemblages for the pre- and post-MWP 1A sea-level positions are illustrated by the horizontal green bands. The resulting extreme bounds for the MWP-1A amplitude (12 and 22 m) are also indicated (green arrows). Several arguments given in the SI suggest that these conservative estimates can be trimmed between 14 and 18 m (brown bands and arrows).

Figure 3: Relative sea-level records over the 16.5 to 12.0 ka BP time window. **(a)** Barbados RSL record based on U-Th dated corals (mainly *A. Palmata*)[19,29]. **(b)** Pacific RSL records. Red circles: Huon Peninsula record[31,32] (Papua New Guinea) based on U-Th dated corals. Purple point: Sunda shelf record[8] based on ^{14}C-dated organic material found in sediment cores (recalibrated using IntCal09[30]; plotted errors are 1σ). The blue rectangle indicates the drowning of a Hawaiian reef 14.7 ka ago[15]. **(c)** Tahiti RSL record based on U-Th dated corals collected in holes drilled onshore (grey symbols)[14,24] and offshore (coloured symbols, this study). **(d)** Rate of glacial melt-water discharge (expressed in mm/yr and Sv) derived from the ESL curve determined by GIA model (see SI and Fig. S11) adjusted to account for the newly obtained timing and magnitude of MWP-1A from Tahitian sea-level observations. **(e)** $\delta^{18}O$ record of the North GRIP Greenland core plotted on its most recent time scale[34]; B: Bølling; OD: Older Dryas; A: Allerød. All depths have been corrected for subsidence (Tahiti) and uplift (all other sites) as described in [24]. For Tahiti and Barbados records, only samples that delineate the upper envelope are shown. Gray lines correspond to linear fits of sea-level data[24]. Greenish and bluish shaded time windows correspond to MWP-1A chronozones inferred from the Barbados record and the Tahiti record (Fig. 2), respectively.

Fig.1

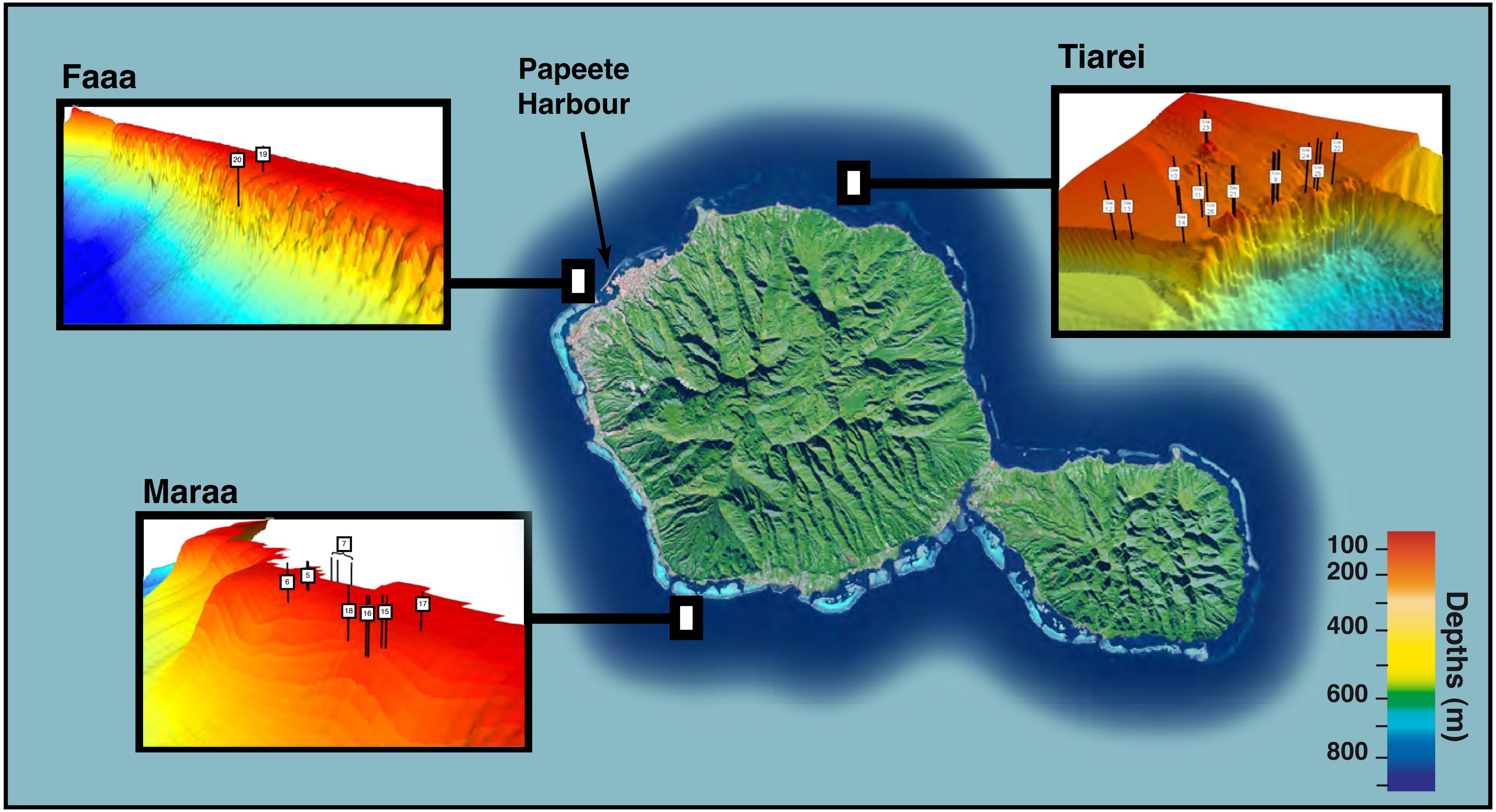

Faaa
Papeete
Harbour
Tiarei
Maraa
100
200
400
600
800
Depths (m)

Fig.2

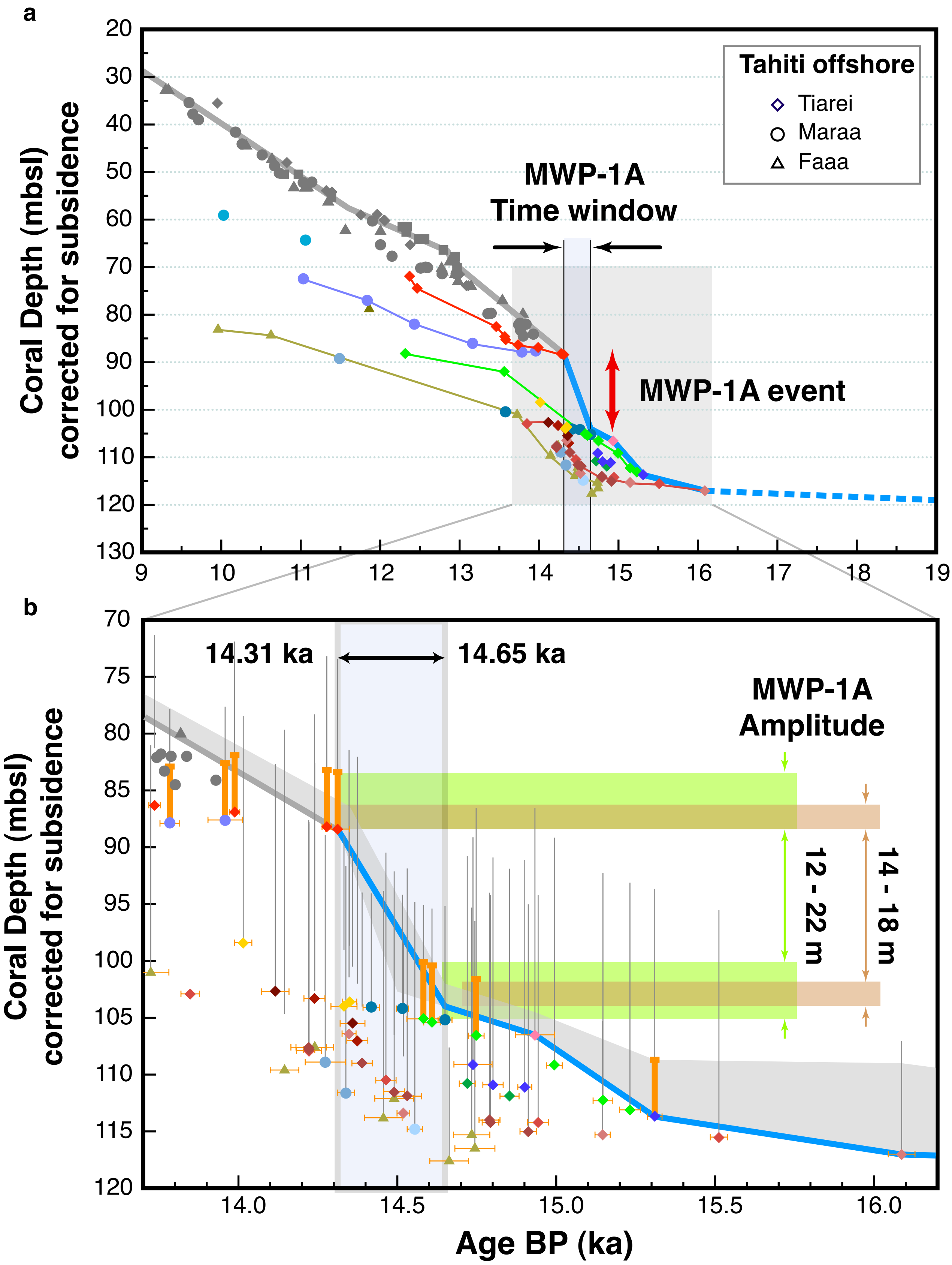
a
b
Coral Depth (mbsl) corrected for subsidence
Tahiti offshore
Tiarei
Maraa
Faaa
MWP-1A
Time window
MWP-1A event
14.31 ka
14.65 ka
MWP-1A
Amplitude
12 - 22 m
14 - 18 m
Age BP (ka)

Fig. 3

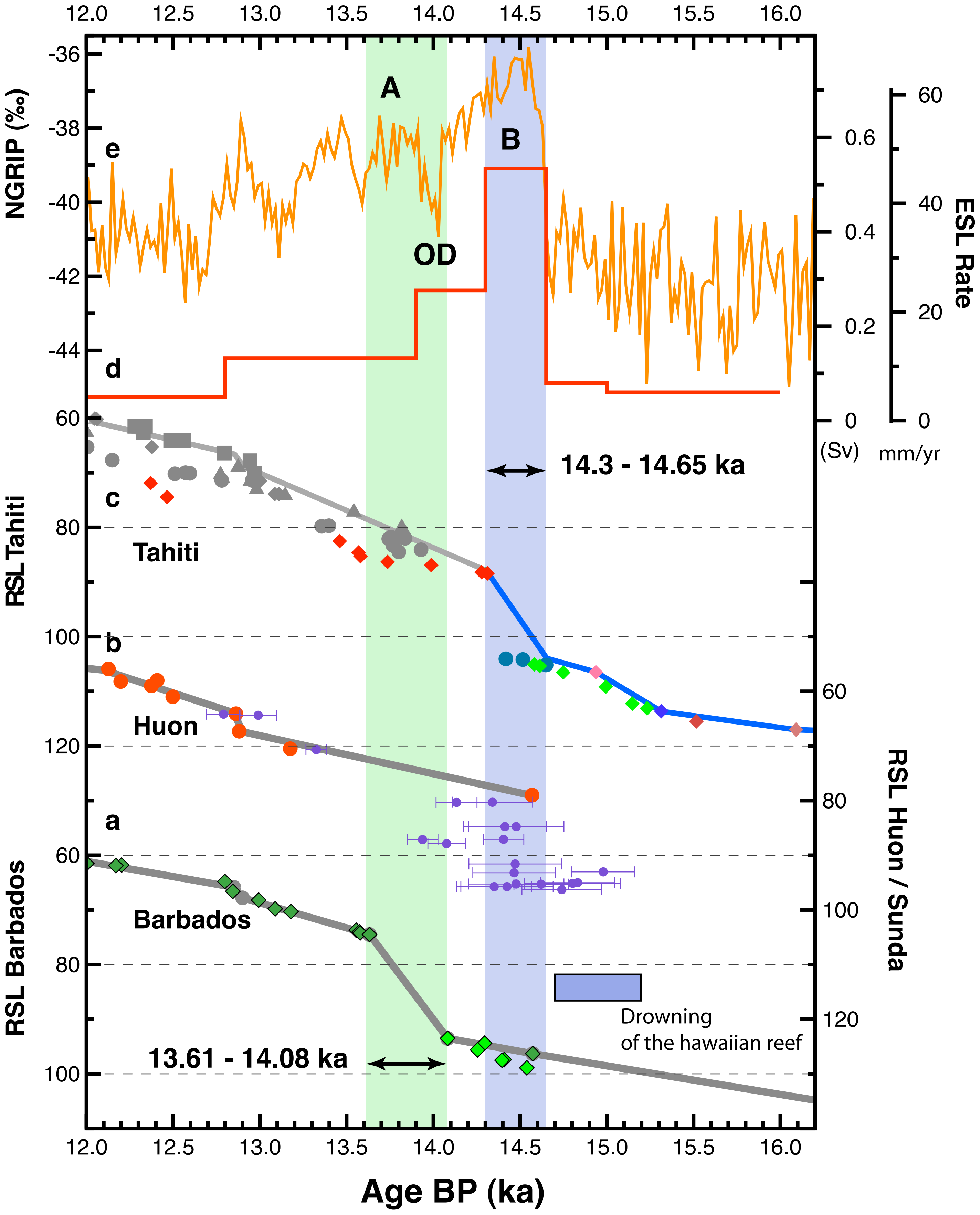
NGRIP (‰)
ESL Rate
(Sv)
mm/yr
RSL Tahiti
RSL Huon / Sunda
RSL Barbados
A
B
OD
e
d
c
b
a
Tahiti
Huon
Barbados
14.3 - 14.65 ka
13.61 - 14.08 ka
Drowning
of the hawaiian reef
Age BP (ka)
12.0
12.5
13.0
13.5
14.0
14.5
15.0
15.5
16.0